Development of a Cable Actuator Test Rig for Identification of Dynamic Running Properties of Synthetic Fiber Ropes

Entwicklung eines Seilwindenprüfstands zur Identifikation dynamischer Laufeigenschaften von Kunststofffaserseilen

Thomas Reichenbach
Felix Trautwein
Andreas Pott
Alexander Verl

Institute for Control Engineering of Machine Tools and Manufacturing Units (ISW)
Faculty for Engineering Design, Production Engineering and Automotive Engineering
University of Stuttgart

Synthetic fiber ropes are being used more frequently in industrial machines and applications due to their low mass, high breaking loads, and compact storage. While the properties of wire ropes, such as breaking load and durability, can be investigated using industrially established test methods, the use of synthetic fiber ropes requires a systematic evaluation of the static and dynamic properties. The cable actuator test rig developed in this work will therefore be used to investigate cable slip as well as friction under highly dynamic motions. Two preload control methods were developed for the test rig so that a cable running on a drum can be tested with various motion and load profiles. The experimental investigations show that the cable slip is dependent on its speed and force, and that operating points with low cable slip can be identified. Furthermore, a Coulomb-viscous friction curve and a direction-dependent efficiency of the tested winch were determined.

[Keywords: test rig, winch, control, preload, cable robot]

Kunststofffaserseile werden aufgrund ihrer geringen Eigenmasse, hohen Bruchlasten und der kompakten Speicherung immer häufiger in industriellen Anlagen eingesetzt. Während die Eigenschaften von Drahtseilen, wie Bruchkraft und Lebensdauer, mit industriell etablierte Prüfverfahren untersucht werden können, erfordert die Verwendung synthetischer Faserseilen eine systematische Bewertung der statischen und dynamischen Eigenschaften. Mit dem in dieser Arbeit entwickelten Seilwindenprüfstand sollen daher der Seilschlupf sowie die Reibung unter hochdynamischen Bewegungen untersucht werden. Für den Seilwindenprüfstand wurden zwei Verfahren einer Verspannungsregelung entwickelt, damit das auf einer Trommelwinde laufende Seil mit Bewegungs- und Lastprofilen geprüft werden kann. Die experimentellen Untersuchungen zeigen, dass der Seilschlupf abhängig von der Seilgeschwindigkeit und -kraft ist und Betriebspunkte mit geringem Seilschlupf identifiziert werden können. Weiterhin wurde ein Coulomb-viskoser Reibverlauf sowie ein richtungsabhängiger Wirkungsgrad der geprüften Seilwinde beobachtet.

[Schlüsselwörter: Prüfstand, Seilwinde, Regelung, Verspannung, Seilroboter]

1 INTRODUCTION

For tasks which require long distance motions like handling tasks, usually, rack-and-pinion drives or linear direct drives are used due to their high position accuracy of a few micrometers. However, the solidly built components usually lead to high moving masses and consequently to a low acceleration capacity. Portal systems are a suitable example for these applications. Using synthetic fiber ropes (following denoted as cables) as linear drive elements, the ratio of mass to payload can be highly increased. These properties become particularly apparent with the use for cable robots: High speeds (>10 m/s) and accelerations (>200 m/s²) [1] as well as long ranges (>10 m) [2] open up new possibilities for the handling and automation of large-scale objects.

1.1 DRIVE SYSTEMS OF CABLE ROBOTS

The control of the position and orientation of a platform of a cable robot is achieved with cables that are driven by a cable actuator system. The positioning accuracy of the cables has a significant influence on the operating characteristics of a cable robot. In addition, the use of winches as drive elements for parallel robots leads to non-linear motion and load profiles, compared to conventional drive systems like hoists for elevators. This is due to the geometric relationships between the spatially manipulable robot platform and the one-dimensional motion of the drives. Another remarkable effect of the flexibility of cables and the winding process itself is, that in dependence of the platform

motion the pretension of the wound cables is unknown and varies, which also induces considerable inaccuracies. Figure 1 shows an example of a measured motion and load profile of a winch during a handling task of a cable robot.
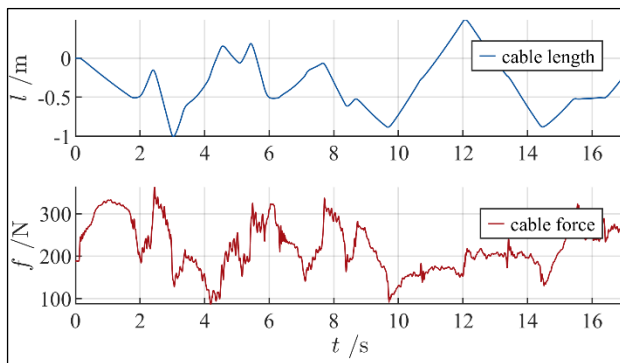

Figure 1.   Path and load profile of a winch for a typical handling task of a cable robot.

Other reasons of the large positioning errors are a combination of mechanical, electrical, and thermal effects of the running cable which have not been investigated so far. The resulting cable slip and the frictional forces can only be measured using very complex measurement technology on the cable actuator or the robotic platform. Since at least seven winches are required for a completely restrained cable robot, this leads to considerable additional expense. Consequently, compensation of the cable slip with model-based control methods on the cable actuator is necessary. To lay a basis for modelling of these effects, a cable actuator test rig was developed and set up at *ISW*. By using this test rig, the dynamic properties of the running cables are investigated. From the experimental investigations, physical cable slip and friction models of the cable actuator will be developed, which has to be integrated as observers in the drive control in order to be able to increase the positioning accuracy.

1.2   STATE OF THE ART

Existing work of the current research investigate durability and lifetime of running high-modulus fiber ropes. For example, Novak [3] identifies factors influencing the durability and develops a general method for estimating the lifetime of different rope types depending which cable actuator is used. With the result, cables could be used industrially for lifting motions in storage technology [4]. Wehr [5, 6] also investigated the lifetime of synthetic fiber ropes in connection with their use in cable robotics under highly dynamic loads. In addition to conventional testing techniques (fatigue bending and tension swell tests), a special high-dynamic test rig was set up, with which bending speeds of 10 m/s can be achieved. The bending speeds are many times higher than with conventional bending machines, which reach approx. 0.2 m/s. At both test methods, the load of the cable is kept constant during the experiments. The focus of the mentioned works above lies mainly on lifetime estimation and the investigation of wear behavior. For the

use of synthetic fiber ropes in robotics, lifetime plays a subordinate role since the maintenance of dynamic limits during platform motion is a decisive process-relevant factor. One relevant property, for example, is the position accuracy of a running cable on a drum, which is being investigated in detail by Schmidt and Pott [7]. Hereby, the test rig consists of two winches to preload a cable. Both winches have integrated force sensors to measure the cable forces. The cable position is measured by an optical coordinate measuring system (laser tracker) and can be moved over a distance of about 5.7 m. The experiments were performed with randomized speeds and forces. The results show that the applied cable force has a high influence on the positioning accuracy. The low stiffness and the ovalization of the cable on the drum are named as possible causes. Furthermore, it is suspected that the force with which the cable is stored on the drum has further influences on the accuracy. Miermeister et al. [8] also investigates the influence of the cable force on the position accuracy and models a hysteresis effect based on load-elongation experiments. The results show that the cable force significantly depends on the winding on the drum with nonlinear forces and velocities generated by a cable robot. Schmidt [9] and Piao et al. [10] describe the creep effects of synthetic fiber ropes and their effect on a platform of a restrained cable robot. The modeling is based on quasi-static measurements with constant load through weights. It is assumed that creep effects also affect the accuracy of running cables. Thus, this paper describes the development of a test rig that can be used to investigate the described deficits in the case of unknown dynamic disturbance influences such as rope slip, friction, or creep effects for running synthetic fiber ropes.

CABLE ACTUATOR TEST RIG

For the modeling of the dynamic running properties and for the subsequent parameter identification, a cable actuator test rig (*CATi*) was developed and set up at *ISW*, with which synthetic fiber ropes can be actuated with load and motion profiles. The test rig with the main components and the sensor systems is shown in Figure 2 and the corresponding data of the drive system and drum are listed in Table 1.

The application of load profiles over large cable lengths requires an additional winch with auxiliary gear. Thus, a preloading test rig with drive redundancy by two winches was built, which can actuate the cable in one direction of motion. Other use cases of preloading test rigs are the investigation of control characteristics and efficiency of automotive gears [11] as well as to identify hysteresis effects for cycloidal gears of industrial robots [12]. However, for *CATi*, drums are needed as additional transmission elements to transfer the rotational motion of the motor into a linear motion of the cable. The test rig therefore consists of two winches: A test winch, which is used to measure the slip and friction characteristics, and a load

winch, which is used to apply the load profiles. The drums are designed with a round groove and spooling traverse with integrated force sensors so that the cable can be unwind and rewind in a single layer. By storing the cable in a single layer on the drum, complex interference effects, as occurs with multi-layer storage [13], are avoided. With the

modular measuring platform between the test and load winch, additional sensors, or test elements such as deflection pulleys can be easily attached.
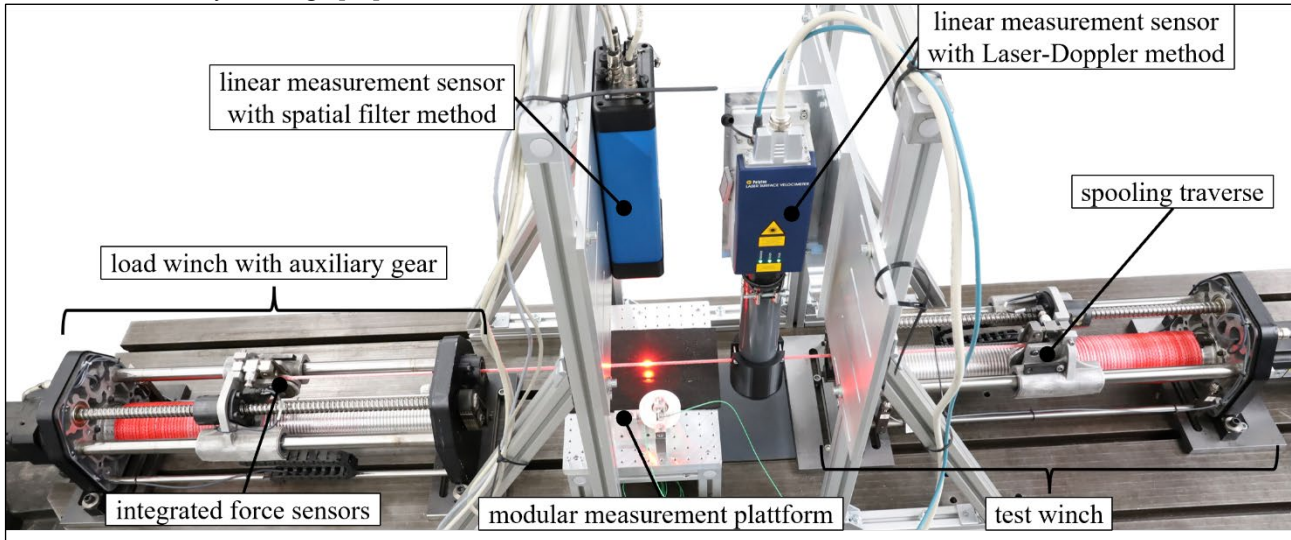

Figure 2.   Cable Actuator Test Rig (CATi)

Table 1.   General data of CATi and drive systems

Parameter	Value	Unit
General Data		
Max. cable length l_{Max}	20	m
Max. cable velocity v_{Max}	5	m/s
Max. cable force f_{Max}	200	N
Synthetic Fiber Rope	**Liros D-Pro 01505-0600**	
Cable diameter d_S	6	mm
Nominal drum diameter D_T	100,36	mm
Groove diameter d_R	6,36	mm
Groove pitch p_R	7	mm
Synchronous Motor	**Rexroth MSK061C-0600**	
Continuous torque τ_C	8	Nm
Max. torque τ_{Max}	32	Nm
Torque constant K_M	1,14	NmA^{-1}
Max. speed n_{Max}	6000	min^{-1}
Planetary Gear	**Rexroth GTE 120**	
Ratio i_P	1:5	-
Nominal efficiency η_G	0,98	-

1.3 MEASURING DEVICES

In order to precisely measure the cable slip, optical sensors are used, which are mounted between the two winch systems. Hereby, the cable slip is defined as the difference between the motor position and the cable position. The reason for installing two sensors with different measuring methods was to verify the output signals. The non-contact optical measurement avoids additional friction and

thus does not influence the motion of the cable. The output signal of the linear measuring sensors is a standardized encoder signal (RS422) from which the velocity and acceleration can be derived in time. In addition to the motion quantities, also the effective cable forces can be measured with an integrated force sensor in the spooling traverse of the winches.

1.3.1 LINEAR MEASURING SENSORS

As mentioned, due to the optical measurement principle the sensors work contactless and thus, the influences on the cable are avoided entirely. The characteristics of the linear measuring sensors used in the *CATi* are listed in Table 2.

Table 2.   Properties of the used linear measuring sensors AS-COspeed and LSV-2100

Property	ASCOspeed	LSV-2100	Unit
Max. velocity	50.00	128.30	m/s
Max. acceleration	400	N/A*	m/s²
Output rate of the encoder interface	500	500	kHz
Absolute accuracy	0.05	0.05	%
Repeatability	0.02	0.03	%
Parameterized encoder resolution	0.02	0.02	mm

*not available

The *ASCOspeed* sensor from TB Sensor uses the spatial frequency filter method. Here, the velocity of the running

cable is mapped onto a differential grid consisting of semiconductor elements. Position data are calculated by filter and integration methods and output as incremental encoder pulses with up to 500 kHz. To verify the measurement data and the slip behavior, the motion data of the cable are additionally measured with a laser surface velocimeter *LSV-2100* from Polytec. The measurement is based on the Laser-Doppler method.

1.3.2 FORCE SENSORS

For single-layer storage, the running cable is guided via a pulley in the spooling traverse. The integration of a force sensor via this existing deflection mechanism is beneficial, since only a few additional components are required. The mechanics of the integrated force sensor are shown schematically in Figure 3. F2306 compression force transducers from Tecsis (WIKA) with a thin-film sensor and a measuring range of up to 2 kN are used for force measurement. The sensor mounting in the rocker and traverse is modular, so that it can be easily replaced by sensors with a different measuring principle, for example piezo sensors.
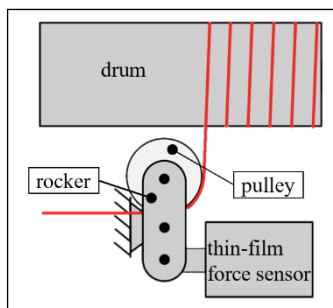

Figure 3. Schematic illustration of the integrated force sensor (edited, [14])

1.4 CONTROL SYSTEM ARCHITECTURE

The used components of *CATi* are mainly standard industrial control technology and thus, allow for reliable and representative statements about the characteristics of running cables. The main components are drive components from Bosch Rexroth and the conversion of measurement data using hardware modules from Beckhoff. TwinCAT 3.1 is used as the automation software, since software modules, for example new model-based control methods, can be integrated via the open control architecture. Figure 4 shows the principle of the control system and the data exchange of the individual components (drives, sensors, peripherals) via the bus system used.

A user can operate the winch test stand via graphical user interface (HMI) with standardized NC commands according to DIN 66025. The control system includes a CNC core, which allows the drives to be moved with jerk-limited seven-phase path profiles. The power for the drives is provided by corresponding power and control components

(motion). The measured data from the drive encoders and linear measuring sensors are transmitted over a serial connection to the input and output components (I/O) and converted to the field bus signal. The analog measured values of the force transducers are also converted into the fieldbus protocol. In this way, drive and sensor data are recorded via the controller in a time-synchronous and real-time manner, enabling the computation of slip and friction caused by the running cable on the drum.
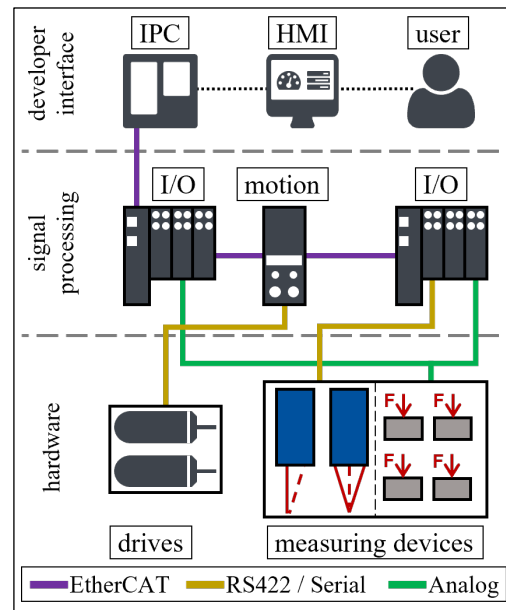

Figure 4. Principle of the control system

2 PRELOAD CONTROL

To move the test winch with a defined load and motion profile, a preload controller is required. Therefore, the cable force is generated by the two redundant drives. In terms of running cables, the work of Hofmann [15] should be mentioned here, in which the lifetime of a multi-layer stored steel ropes was increased with the generation of a constant preload by an additional traction sheave. However, *CATi* requires the application of dynamic loads and the compensation of disturbance effects, so that the preload control loop must be closed under the existing cascade control of the drives. Two options are available for integrating the preload controller: Preloading the cable via a speed offset or a torque offset. In the following subsections, these two control methods are described as velocity-based and torque-based preload control.

2.1 VELOCITY-BASED PRELOAD CONTROL

Figure 5 shows the velocity-based preload control as a block diagram. The position specification is made with the target cable length l_d, which is calculated with a constant gear ratio $i_{G,1} = 180°/(\pi D_T)$ of the test winch to the required drive position $\varphi_d = l_d i_{G,1}$. In addition, a velocity

feedforward is used to increase the bandwidth of the preload control. The target speed is calculated with a P position controller with amplification factor K_v to

$$\omega_{d,i} = K_v(\varphi_d - \varphi_1) + \frac{d\varphi_d}{dt} , \qquad (1)$$

and transferred to the drive control of the load winch. The index $i = 1$ is used for the test winch and $i = 2$ for the load winch with auxiliary gear. In addition, a motor speed offset ω_f is generated by the preload controller and added to the actual motor speed $\omega_{m,i}$ and to the target motor speed $\omega_{d,i}$ of the respective drive. The target motor torque is computed with

$$\tau_{d,1} = K_p(\omega_{d,1} - \omega_{m,1} - \omega_f) + \frac{1}{T_n} \int (\omega_{d,1} - \omega_{m,1} - \omega_f) dt . \qquad (2)$$

For the load winch, the gear ratio $i_{G,2} = 180°/(\pi i_p D_T)$ must be considered in formula (2). The target torque $\tau_{d,1}$ is converted to a proportional target motor current by the torque constant K_M and used for the PI current controller. The field control used for synchronous motors is not described in more detail here, since it is subordinate to the

preload control. The cable actuator dynamics includes the power unit of the motor L_i, the winch dynamics W_i as well as additional disturbances z_i caused by additional drive elements, such as the motion transmission to the spooling traverse. The yet unknown system behavior of the running cable, which are to be investigated with the *CATi*, are denoted as C in the block diagram. A PID controller is used for preload control, which compensates the error between a user-specified target cable force f_d and the measured cable force f computes a motor speed offset with

$$\omega_f = K_{pf}(f_d - f) + \frac{1}{T_{nf}} \int (f_d - f) dt + T_{vf}\frac{d(f_d - f)}{dt} . \qquad (3)$$

Based on the target cable force, the gear ratios are also used to feedforward the torque in the respective drive control, which relieves the PID controller. The velocity-based preload is beneficial because the drive of the test winch can be controlled to positions specified by the user. Statistical calculations of the cable slip can be calculated based on unique positions of the drum.
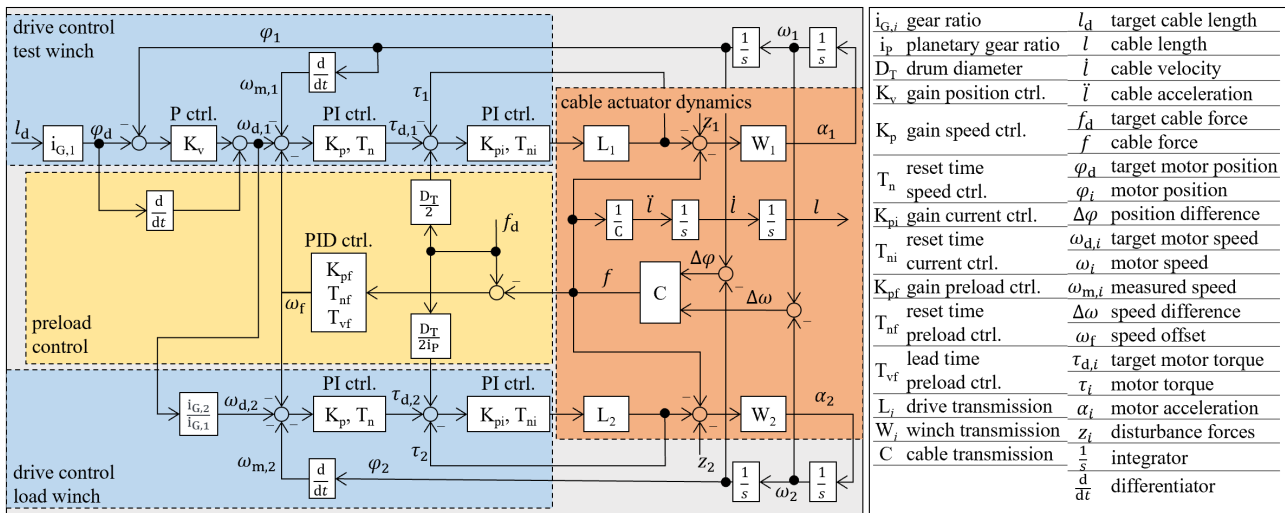

Figure 5.   Velocity-based preload control (with $i = 1$ for the test winch und $i = 2$ for the load winch)

2.2 TORQUE-BASED PRELOAD CONTROL

The behavior of the velocity-based preload control influences the drum speed and thus also the speed of the running cable. Since it is assumed that the cable slip is also velocity-dependent, the generated offset of the speed-based preload control also affects the measurement of the slip. Therefore, a second control scheme is developed that generates the preload by the motor torque. The block diagram of the torque-based preload control is shown in Figure 6.

For preloading the cable, the position control loop of the test winch is cut and controlled to the motor target speed $\omega_{d,1}$ generated from the motion profile. The load winch is controlled to a target torque $\tau_{d,2}$, which is calculated with the target cable force f_d, the gear ratio of the planetary

gear i_p, the drum diameter D_T, and the gain feedforward factor K_{ff} and added to a cable force generating target torque of the test winch $\tau_{d,1}$. Thus, the target torque of the load winch can be computed with

$$\tau_{d,2} = K_{ff}\frac{D_T}{2i_p}f_d - \tau_{d,1} . \qquad (4)$$

A PID controller is also used for preload control, which compensates for disturbance forces z_i and transmits a torque offset τ_f to the load winch as output. The calculation of the torque offset is analogous to formula (3). Since the preload is generated with this type of control via the torque of the drives, the errors due to the drum speed on the cable slip is decreasing.
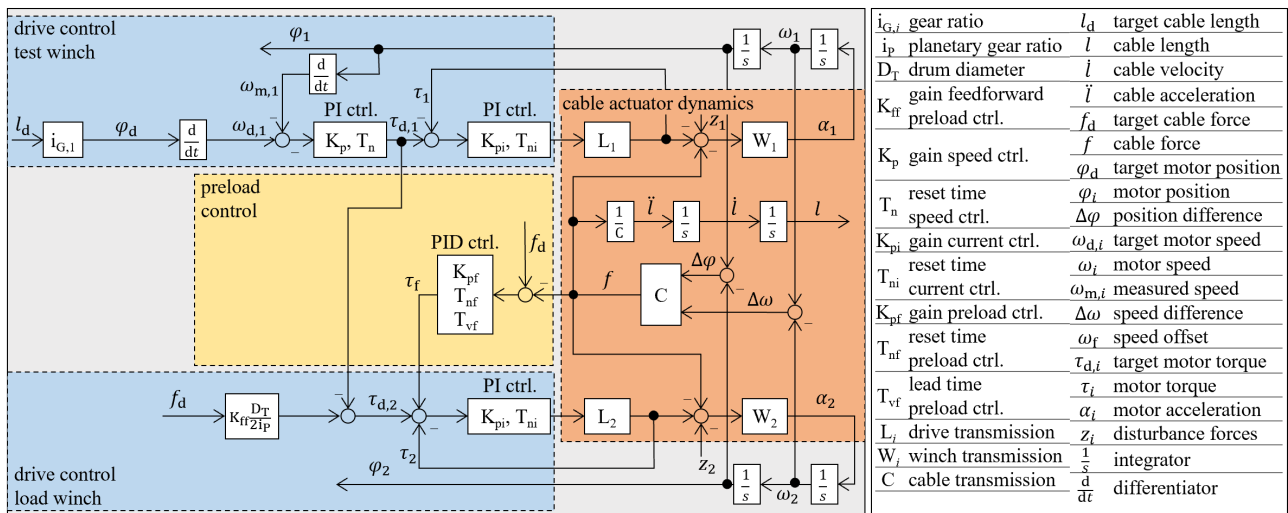
Figure 6. Torque-based preload control (with $i = 1$ for the test winch und $i = 2$ for the load winch)

3 EXPERIMENTAL VALIDATION

3.1 EXPERIMENTAL DESIGN

The developed winch test rig will initially be used to investigate cable slip and friction occurring in the test winch in detail. To reduce complex interference effects due to the mass inertias and for initial modeling approaches, the experiments will be carried out at steady state with constant cable forces and drum speeds. Table 3 lists data on the experiments. For statistical evaluation, each series of measurements includes a number of k_T measurements. The sensor data are recorded over the measurement length l_M with constant cable force f_d and constant cable speed $\dot{l}_d = \omega_{d,1} D_T \pi / 180°$.

Table 3. Experimental design

Parameter	Value	Unit
Number of measurements k_T	10	-
Measured cable length l_M	10	m
Cable forces f_d	[70, 125, 180]	N
Cable velocities $\dot{l}_d$	[-5, -2, -0.5, 0.5, 2, 5]	m/s
Preload control methods	velocity-based torque-based	-

The series of measurements are repeated for the two developed control methods to investigate the influence of the speed offset by the controller on the cable slip. Finally, a total of 360 measurements were performed. In the following sections, negative cable velocities are referred to as "rewind" and positive cable velocities as "unwind".

3.2 EXPERIMENT EXECUTION

The tests are carried out with the control parameters listed in Table 4. Within the scope of this work, only the synthetic fiber rope Liros D-Pro 01505-0600 is investigated, since it also used for the cable robot COPacabana [16] available at *ISW*. To be able to model the running properties of the cable as accurately as possible, other cable types will be investigated for future measurements: a high-strength polyester rope braid with TPU sheath and a rope braid with Vectran HT T90. For the experiments, the test rig is moved with a jerk-limited path profile. After the acceleration phase, the drum speed is kept constant. To reduce the influence of previously performed measurement series and to ensure a consistent initial situation for each measurement, an initial winding process with the given combination of velocities and cable forces was performed. This procedure ensures that each measurement starts at the same initial condition. The measurement data are recorded over the measurement length l_M from a start position of 4 m to an end position of 14 m. Then, the recording is terminated, and the deceleration phase begins. The measurement data and evaluation scripts can be reviewed and downloaded via the Data Repository for Research Data at the University of Stuttgart [17].

Table 4. Control parameters for the experiments

Parameter	Drive Control		Unit
	Test Winch	Load Winch	
K_v	1	2	1000/min
K_p	1,5	0,5	Nm/(rad/s)
T_n	10	5	ms
K_{pi}	9	9	V/A
T_{ni}	4	4	ms

	Preload Control		
	ω-based	τ-based	
K_{ff}	0	1,5	-
K_{pf}	0,001	0,01	s/N | m
T_{nf}	0	100	ms
T_{vf}	0	50	ms

ω: motor speed, τ: motor torque

4 DISCUSSION

4.1 ANALYSIS

The cable slip Δl_S is calculated with the difference of motor position φ_1 and the cable position l measured with the linear measurement sensors:

$$\Delta l_S = l - \varphi_1 \frac{\pi}{180°} D_T . \qquad (5)$$

Cable slip results from unconsidered parts of the cable's motion transmission in the ratio, which is usually assumed to be a constant factor in drive control. For wire ropes, for example, slip is taken into account for the design of traction sheaves and divided into sliding, running radius and elongation slip [18]. In addition, the speed error e_ω is calculated with

$$e_\omega = (\omega_{d,1} - \omega_1) \frac{\pi}{180°} D_T , \qquad (6)$$

to verify the influence of the speed offset generated by the preload control to the motor speed controller. Since the speed is differentiated from encoder positions, the noisy signal is processed with an FIR filter.

The total friction $f_{R,Total}$ of *CATi* is calculated with the difference of the measured drive torques τ_i:

$$f_{R,Total} = |\underbrace{\frac{2i_P}{D_T}\tau_2}_{f_L} - \underbrace{\frac{2}{D_T}\tau_1}_{f_T}| . \qquad (7)$$

Since the preload control generates an additional speed or torque offset on both drives, the proportional friction forces of the test and load winches are formulated as a constrained nonlinear function and which is solved using the interior-point method [19] with MATLAB 2022b. The optimization problem is formulated as

$$\min_{[f_{R,L}, f_{R,T}, \lambda]} y = \left(f - \left(\lambda \cdot (f_L - f_{R,L}) \right) + (1 - \lambda)(f_T - f_{R,T}) \right)^2 \qquad (8)$$

$$\text{subject to } \underbrace{f_{R,T} + f_{R,L}}_{f_{R,Total}} = |f_L - f_T|$$

$$f_{R,T} \leq f_{R,L} \leq f_{R,Total}$$

$$0 \leq \lambda \leq 1 .$$

Here, $f_{R,T}$ is to the friction force of the test winch, $f_{R,L}$ is the friction force of the load winch, and λ is the distribution factor of the of the forces generated by the motor torques. For the constraint $f_{R,T} \leq f_{R,L}$ the assumption is made that the friction forces of the load winch are higher than those of the test winch due to the additional auxiliary gear.

Friction in the drive system of the winch causes power losses which influence the efficiency factor. *CATi* will also be used to investigate the overall efficiency which is calculated with

$$\eta_{Total} = \frac{\overbrace{\frac{P_{Cable}}{f \cdot l}}}{\frac{P_T + P_L}{P_{Mech}}} . \qquad (9)$$

Here, P_{Cable} is the mechanical power of cable motion and P_{Mech} is the total input drive power by two motors of the test winch P_T and load winch P_L.

Each measurement series is averaged over ten measurements and the standard deviation is calculated over the entire measurement length l_M. To compare the standard deviation over the measurement series, the averaged standard deviations for cable slip $\bar{\sigma}(\Delta l_S)$, total friction $\bar{\sigma}(f_{R,Total})$, and cable force errors $\bar{\sigma}(e_f)$ with $e_f = (f - f_d)$ are calculated (see Figure 7).
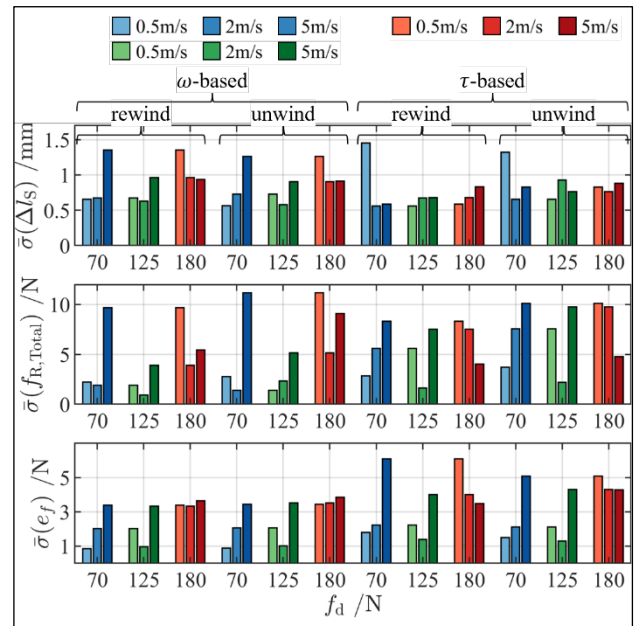

Figure 7. Mean standard deviations of cable slip $\bar{\sigma}(\Delta l_S)$, total friction $\bar{\sigma}(f_{R,Total})$, and cable force errors $\bar{\sigma}(e_f)$ for cable forces f_d and cable velocities $\dot{l}_d$

4.2 RESULTS

Figure 8 shows the cable slip and speed error of the measurement series with speed-based preload control. The cable slip is shown over the target cable length $l_d = 0 \cdots l_M$. The dependence of the slip on the applied cable force, the cable speed and the direction of motion can be observed. At cable forces of $f = 70$ N a positive slip is observed, which decreases with increasing forces and becomes negative at $f = 180$ N. A negative slip means that the motors reduce their position difference to reach the target cable force. Conversely, a positive slip corresponds to an increase in the position difference of the motors. To achieve the lowest possible cable slip, it is assumed that running synthetic fiber rope must have a suitable operating point at defined loads and velocities. Furthermore, an integral progression of cable slip can be seen, as it increases with increasing cable lengths. This suggests that an offset in cable

velocity leads to an increasing slip. Thus, controlling the load via the speed offset will transfer additional drum speed errors to the cable. As already explained in section 2.2, the torque-based preload control was developed to reduce the influence of speed offset on the slip measurement.
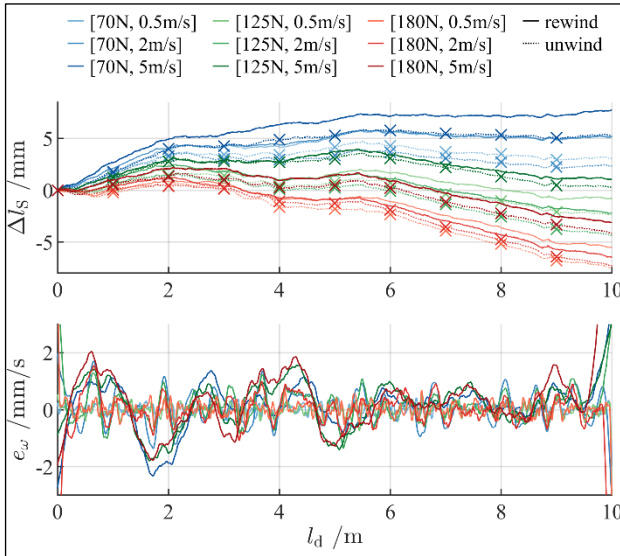

Figure 8.   Cable slip Δl_S (top) and motor speed error e_ω (bottom) averaged over the measurement series with velocity-based preload control

The measurement results with torque-based preload control are shown in Figure 9. To validate that an additional speed offset influences the slip, the speed error of the test winch is shown in the lower graphs. The sharply rising and falling curves for cable lengths up to ~0.5 m and from ~9.5 m, respectively, result from the filtering method used.
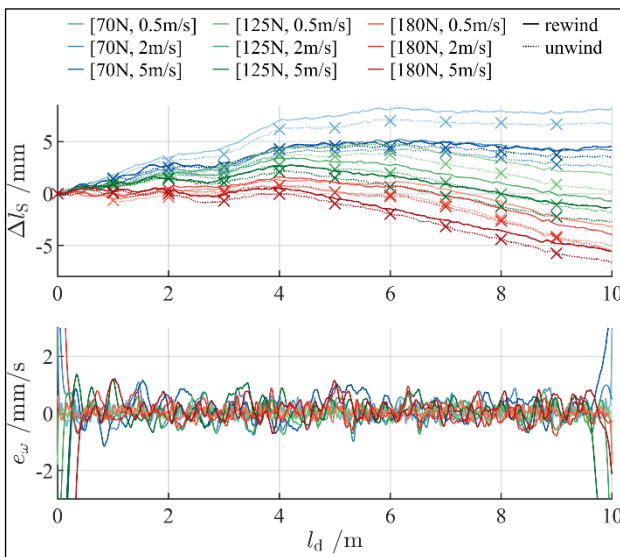

Figure 9.   Cable slip Δl_S (top) and motor speed error e_ω (bottom) averaged over the measurement series with torque-based preload control

The speed errors of the torque-based preload control are approx. 50% lower than those of speed-based preload control, which means that the measured cable slip also shows changed courses at the same cable forces and velocities. It can also be observed with torque-based preload control that positive slip occurs at low cable forces and negative slip at high cable forces. Furthermore, an integral course of the curve can also be seen.

In addition to slip investigations, friction is also to be investigated. Figure 10 shows the friction forces calculated with formula (8) and (9) as well as the total efficiency of *CATi*. Since the experiment comprises measurement series with three cable forces and six velocities, the measurement points were extrapolated. As an example, only the friction forces and efficiencies for torque-based preload control are shown, since the measuring points for speed-based preload control show a very small deviation.
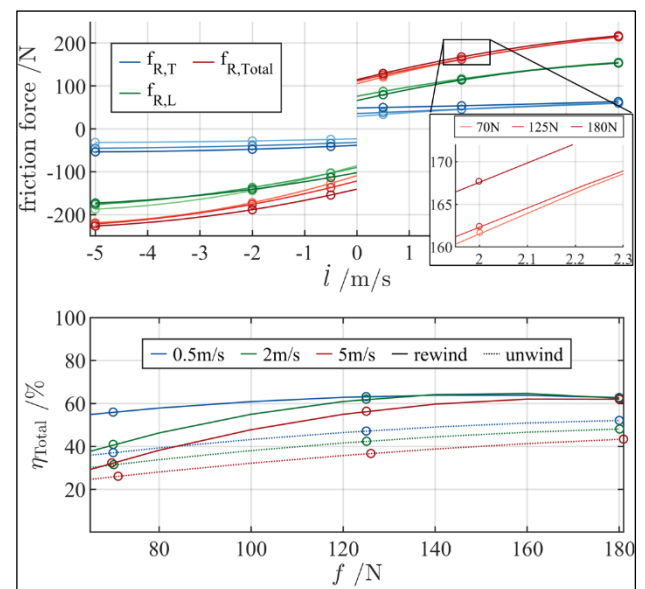

Figure 10. Total friction $f_{R,Total}$, friction of the test winch $f_{R,T}$, and friction of the load winch $f_{R,L}$ at different cable forces (top), and efficiency factor of CATi (bottom)

The frictional force of the load winch $f_{R,L}$ has the largest amount of the total frictional force, which can be explained by additional auxiliary gears in the drive train. The frictional force of the test winch $f_{R,T}$ is comparatively small, so that it can be assumed that the auxiliary gear causes the difference in frictional force. The cable force for preloading the cable has a lesser influence on the friction. The friction force differences are greatest in the range of static friction, which must be considered for future experiments. Measurement inaccuracies can also cause the differences in friction force since the mean standard deviation has a similar value. In the viscous friction range, the curves with different cable forces converge.

For the overall efficiency, direction-dependent power losses are observed. Higher power losses can be observed

when the test winch is unwinding compared to rewinding. As expected, the efficiency increases with increasing cable force and decreases at higher cable velocities due to power losses caused by viscous friction.

5 CONCLUSION AND OUTLOOK

In this paper, a novel cable actuator test rig for the investigation of cable slip and friction of running synthetic fiber ropes was presented. Hardware components, measurement devices, and the control architecture were described. To perform experiments with cable force and position profiles, a speed-based and a torque-based prelaod control were developed. The experimental validation of *CATi* includes series of measurements with constant cable forces and velocities for statistical evaluation. The results of the slip experiments show an increasing curve over the target cable length for both control methods, which can be explained by the cable velocity differences. The friction tests show, as a first approximation, a Coulomb viscous curve and a high friction component of the planetary gear used on the load winch. The amount of friction caused by the preload is greater at low cable velocities of 0.5 m/s than at high cable velocities. Overall, preloading the cable has a minor effect on the winch friction. Furthermore, friction and power losses are dependent on the direction of cable motion. The efficiency during rewinding is ~10% higher than during unwinding of a cable.

In the future, *CATi* will be used to investigate the influence on cable slip due to velocity differences, which may have a major impact. In addition, accelerated path profiles will also be examined. The aim is to develop a dynamics model that can be used as an observer to compensate for the cable slip during operation. For the investigation of the friction forces, additional experiments will be performed. Especially in the area of static friction, it will be investigated which mechanical friction model can be used for winches (for example Stribeck, Coulomb-viscous, or Lund-Grenoble models). The developed models and compensation methods will be validated on *CATi* with different types of synthetic fiber ropes. Further research topics are the transfer of the preload control to other cable actuator systems for running cables with traction sheaves and linear direct drives.

LITERATURE

[1] T. Bruckmann, „Auslegung und Betrieb redundanter paralleler Seilroboter," phdthesis, University of Duisburg-Essen (Uni DuE), Duisburg, Germany, 2010.

[2] M. Fabritius, C. Martin, G. R. Gomez, W. Kraus und A. Pott, „A Practical Force Correction Method for Over-Constrained Cable-Driven Parallel Robots," in *Cable-Driven Parallel Robots* (Mechanisms and Machine Science), M. Gouttefarde, T. Bruckmann und A. Pott, Hg., Cham: Springer International Publishing, 2021, S. 117–128.

[3] G. Novak, „Zur Abschätzung der Lebensdauer von laufenden hochmodularen Faserseilen," phdthesis, Institut für Fördertechnik und Logistik (IFT), Universität Stuttgart, Stuttgart, Germany, 2017.

[4] G. Novak, „Einsatz hochmodularer Faserseile in fördertechnischen Anwendungen am Beispiel eines Regalbediengerätes: Use of high-modulus fibre ropes in rope drives using the example of S/R-machines," *Logistics Journal*, 2016, doi: 10.2195/lj_Proc_novak_de_201605_01.

[5] M. Wehr, „Beitrag zur Untersuchung von hochfesten synthetischen Faserseilen unter hochdynamischer Beanspruchung," phdthesis, Institut für Fördertechnik und Logistik (IFT), University of Stuttgart (UStutt), Stuttgart, Germany, 2017.

[6] M. Wehr, A. Pott und K.-H. Wehking, „Bending Fatigue Strength and Lifetime of Fiber Ropes," in *Cable-Driven Parallel Robots: Proceedings of the Third International Conference on Cable-Driven Parallel Robots*, Quebec City, Canada, C. M. Gosselin, P. Cardou, T. Bruckmann und A. Pott, Hg., Bd. 53, 2018, S. 73–84, doi: 10.1007/978-3-319-61431-1_7.

[7] V. Schmidt und A. Pott, „Investigating the effect of cable force on winch winding accuracy for cable-driven parallel robots," *Proceedings of the Institution of Mechanical Engineers, Part K: Journal of Multi-body Dynamics*, 2015, doi: 10.1177/1464419315586517.

[8] P. Miermeister, W. Kraus, T. Lan und A. Pott, „An Elastic Cable Model for Cable-Driven Parallel Robots Including Hysteresis Effects," in *Cable-Driven Parallel Robots (CableCon 2014)*, Duisburg, Germany, A. Pott und T. Bruckmann, Hg., Bd. 32, 2015, S. 17–28, doi: 10.1007/978-3-319-09489-2_2.

[9] V. Schmidt, „Modeling Techniques and Reliable Real-Time Implementation of Kinematics for Cable-Driven Parallel Robots using Polymer Fiber Cables," phdthesis, University of Stuttgart (UStutt), Stuttgart.

[10] J. Piao, X. Jin, E.-P. Choi, J.-O. Park, C.-S. Kim und J. Jung, „A Polymer Cable Creep Modeling for a Cable-Driven Parallel Robot in a Heavy Payload Application," in *Cable-Driven Parallel Robots: Proceedings of the Third International Conference on Cable-Driven Parallel Robots*, Quebec City, Canada, C. M. Gosselin, P. Cardou, T. Bruckmann und A. Pott, Hg., Bd. 53, 2018, S. 62–72, doi: 10.1007/978-3-319-61431-1_6.

[11] M. J. Imdahl, „Hochgenaue Wirkungsgradbestimmung an Getrieben unter praxisnahen Betriebsbedingungen," phdthesis, Rheinisch-Westfälische Technische Hochschule Aachen (RWTH Aachen), Aachen, Germany, 1997.

[12] P. Mesmer, P. Nagel, A. Lechler und A. Verl, „Modeling and Identification of Hysteresis in Robot Joints with Cycloidal Drives," in *2022 IEEE 17th International Conference on Advanced Motion Control (AMC)*, Padova, Italy, 2022, S. 358–363, doi: 10.1109/AMC51637.2022.9729274.

[13] M. Schulze, „Kompatibilität von Faserseil und mehrlagig bewickelter Seiltrommel: Entwicklung eines Verfahrens zur Analyse, Berechnung, Abstimmung und Qualitätsbewertung der Mehrlagenwicklung," phdthesis, Technische Universität Clausthal (TU Clausthal), 2021.

[14] W. Kraus, M. Kessler und A. Pott, „Pulley friction compensation for winch-integrated cable force measurement and verification on a cable-driven parallel robot," in *Robotics and Automation (ICRA 2015)*, Seattle, WA, USA, 2015, S. 1627–1632, doi: 10.1109/ICRA.2015.7139406.

[15] R. Hofmann und T. Schmidt, „Seilkraftregelnde Hubwerke: Steigerung der Betriebs- und Lebensdauer von Drahtseilen in Mehrlagenwicklung," *Logistics Journal*, 2021, doi: 10.2195/lj_Proc_hofmann_de_202112_01.

[16] F. Trautwein, T. Reichenbach, P. Tempel, A. Pott und A. Verl, „COPacabana: A Modular Cable-Driven Parallel Robot," in *Sechste IFToMM D-A-CH Konferenz*, Lienz, Austria, M. Pfurner und F. Dohnal, Hg., 2020, doi: 10.17185/duepublico/71189.

[17] T. Reichenbach, F. Trautwein, A. Pott und A. Verl. „Measurement data for: Development of a Cable Actuator Test Rig for Identification of Dynamic Running Properties of Synthetic Fiber Ropes."

[18] M. Molkow, „Die Treibfähigkeit von gehärteten Treibscheiben mit Keilrillen," University of Stuttgart (UStutt), Stuttgart, Germany, 1982.

[19] R. H. Byrd, M. E. Hribar und J. Nocedal, „An Interior Point Algorithm for Large-Scale Nonlinear Programming," *SIAM J. Optim.*, Jg. 9, Nr. 4, S. 877–900, 1999, doi: 10.1137/S1052623497325107.

Thomas Reichenbach, M.Sc., Research Assistant at the Institute for Control Engineering of Machine Tools and Manufacturing Units (ISW), University of Stuttgart.

Felix Trautwein, M.Sc., Research Assistant at the Institute for Control Engineering of Machine Tools and Manufacturing Units (ISW), University of Stuttgart.

Prof. Dr.-Ing. Andreas Pott, Professor at the Institute for Control Engineering of Machine Tools and Manufacturing Units (ISW), University of Stuttgart. His research at the ISW focus on cable-driven parallel robots. Furthermore, Andreas Pott is Senior Director for Automation and Digitalization at GEA Group, which is one of the world's largest systems suppliers for the food, beverage, and pharmaceutical industries.

Prof. Dr.-Ing. Dr. h.c. mult. Alexander W. Verl, Chair in Manufacturing Mechatronics and Head of Institute for Control Engineering of Machine Tools and Manufacturing Units (ISW), University of Stuttgart. Alexander W. Verl studied Electrical Engineering at Friedrich-Alexander-University Erlangen-Nürnberg (received the Dipl.-Ing. degree in 1991) and earned his Dr.-Ing. degree in Control Engineering at the Institute of Robotics and Mechatronics (DLR). Since 2005 he is full professor and managing director of the *ISW* at the University of Stuttgart. 1992-1994 he worked as a development engineer at Siemens AG. 1997-2005 he was founder and managing director of AMATEC Robotics GmbH (became part of KUKA Roboter GmbH in 2005); 2006-2014 he was also managing director of Institute at Fraunhofer IPA as an ancillary job. From 2014 to 2016 he was on leave from the University during his time as Executive Vice President of Technology Marketing and Business Models at the Fraunhofer Gesellschaft e.V. Alexander Verl specializes in industrial control technology, mechatronics, robotics, and production IT.

Address: Institut für Steuerungstechnik der Werkzeugmaschinen und Fertigungseinrichtungen (ISW),
Universität Stuttgart,
Seidenstr. 36, 70174 Stuttgart, Germany,
Phone: +49 711 685-84524,
E-Mail: thomas.reichenbach@isw.uni-stuttgart.de